Analyst

PAPER

Cite this: *Analyst*, 2015, **140**, 3535

Fast identification and quantification of BTEX coupling by Raman spectrometry and chemometrics†

J. Moreau and E. Rinnert*

Received 7th January 2015,
Accepted 23rd March 2015

DOI: 10.1039/c5an00035a

www.rsc.org/analyst

Monoaromatic hydrocarbons (MAHs) monitoring is of environmental interest since these chemical pollutants are omnipresent. While waiting for robust sensors able to detect hydrocarbons at very low levels, the present study shows how each compound from pure BTEX mixtures can be identified fast and quantified thanks to Raman spectrometry and data processing based on the SIMPLISMA algorithm. A preprocessing module has been created to remove background contributions and a postprocessing program has been added to achieve matching and calibration. A wide range of BTEX concentrations and relative proportions has been investigated in order to determine the limitations of the processing. Output results achieved an accuracy of up to 95%. This method could be extended to other important pollutants such as polyaromatic hydrocarbons (PAHs) and chlorinated hydrocarbon derivatives.

Introduction

Among the different environmental pollutants, the monoaromatic hydrocarbons (MAH) are among the most common in ground and surface waters. This is due to their presence in petroleum and its derivatives. So the main source of this pollution is known to be the exhaust gas emissions from fuel combustion.[1] MAH generally refers to the so-called BTEX compounds, which are benzene, toluene, ethylbenzene and xylenes (*ortho*-, *meta*-, *para*-isomers); environmental laws and recommendations take them into consideration.[1–4] In addition to the intensive use of fuels, the monoaromatic hydrocarbons play a part of prime importance in industry because they are used as raw materials and solvents in many applications. As a consequence contamination occurs around petroleum and natural gas production and refinery sites including petrol stations, as well as BTEX-consuming industries. Atmospheric fallout, unforeseen or wilful spills and industrial effluents are nothing better than BTEX sources in any environment.

What makes these compounds so intensively studied is their omnipresence combined with their toxicity for both humans and aquatic life. The central nervous system is one of the biological system targets of monoaromatic hydrocarbons. The dangerous neurotoxicity of BTEX comes from their high volatility combined with their easy absorption into lung alveoli and skin, without allowing their favorable miscibility in human biological fluids. After repeated exposure to these compounds, the classic signs due to long term intoxication are expressed by a state of fatigue, anxiety and sleep disturbance and by even nervous breakdowns.[5] The whole BTEX provides more or less serious mutagenic and reprotoxic effects.[6] In the particular case of benzene, the most dangerous of BTEX, long term intoxication specifically borders bone medulla where blood cells are made and can lead to deadly aplastic anaemia and/or leukaemia (carcinogenic Group 1, mutagenic, reprotoxic).

Until now, the analytical standard procedure used for monitoring amounts of BTEX in water consists in taking and gathering water samples for analysis in a laboratory. The analytical process involves different extractions such as Solid Phase (micro)Extraction (SPE) and purge and gas trap chromatography which can be coupled with mass spectrometry.[2,7–9] In spite of the high selectivity and sensibility obtained by these methods, significant disadvantages remain. First, the time lag between the sampling and the analyses that cannot allow sufficient reactivity in case of accidental spill, for example. Then, scientific staff must be highly qualified to collect representative samples without any external contamination and loss of analytes. Several studies have proposed a solution to bypass the SPE step with direct injection[10,11] or the headspace sampler based method.[8,12–18] In the same way, some work has been carried out using HPLC.[19,20] But these systems would be neither easily portable nor *in situ* used. Incidentally, Raman spectrometry was seldom used instead of GC/MS.[21,22]

IFREMER, Laboratoire Détection, Capteurs et Mesures, CS10070, 29280 Plouzané, France. E-mail: emmanuel.rinnert@ifremer.fr

†Electronic supplementary information (ESI) available: Experiment plan tables, computed *via* SIMPLISMA 1 *vs.* actual BTEX concentration figure, complementary data processing result graph. See DOI: 10.1039/c5an00035a

According to these statements, optical remote sensing clearly appears to be a prime technology. Removal of the collecting, sampling and carrying steps represents an indisputable advantage. However, nowadays there is a lack of relevant techniques that allows fast qualitative, quantitative and *in situ* analysis of BTEX. Among the different methods, Laser-Induced Fluorescence seems to be inappropriate in real cases because of the broadness and overlap of output signals.[23] With regard to Infrared Attenuated Total Reflection spectroscopy, results are encouraging even if the spectral range available to identify the pollutants is quite narrow and very often limited to only one or two bands by components.[24,25] Finally Raman spectrometry[26–30] remains very attractive owing to the fact that water response is weak, differentiation of analytes is quite high, and measurements are very fast[31–33] and may be even used without standardization.[34] The main feature to be improved is the sensitivity, which can be done thanks to novel optical fibre probes[35] and SERS substrates,[36–41] while chemometric quantification algorithms,[42–45] when used, are often Partial Least Square-based[30,31,37,46–48] (PLS).

Herein the aim of the study is to determine the feasibility of identification and quantification of BTEX by Raman spectrometry in pure compound mixtures. While waiting for robust SERS sensors able to detect hydrocarbons at very low levels, the present study is focused on how each compound from pure BTEX mixtures can be identified fast and quantified thanks to Raman spectrometry and data processing based on the SIMPLISMA algorithm. As far as we know, only Cooper *et al.* have ever tried to differentiate the 6 BTEX together by Raman spectrometry in order to perform their quantification thanks to chemometrics.[31] This study consists of the comparison of near-IR, mid-IR and FT-Raman spectroscopy combined with PLS processing for the routine determination of BTEX in petroleum fuels. Our complementary study is focused on Raman spectrometry, and the range of concentrations is larger than Cooper's. Finally we use chemometrics based on the SIMPLISMA algorithm.[49] The advantage of this data processing is its interactivity and fast adaptability to new and/or unknown compounds, which is needed in real cases. Indeed, the number of components to be found and isolated from the spectra as well as an offset value to reduce the noise level can be easily modified. Also, if the background contribution is high, a second derivative spectra can be used to get around that. Many methods for background subtraction have been reported[52–58] accompanied with their pros and cons. Here baseline contributions are not huge and spectra were pre-processed for both band shift corrections, as it can affect the data analysis,[50] and background removal according to Eilers' approach.[51]

Moreover in the future, inevitably more and more data will be demanded by health organizations or simply by the monitoring of a mounting number of places in order to increase pollution mapping precision. In this way it is obvious that the fastest method to obtain qualitative and quantitative results will be needed. It would be even better if it could be remote-controlled, which Raman spectrometry coupled with chemometrics would enable.

Experimental

Chemicals and sampling

All the compounds were purchased from Sigma-Aldrich – benzene (≥99%), toluene (≥99.5%), ethylbenzene (≥99%), *ortho*-xylene (≥99%), *meta*-xylene (≥99%), *para*-xylene (≥99%), chloroform (≥99.5%). The different mixtures were prepared by adding the desired volumes of the different components thanks to suitable micropipettes – 2–20 μL, 20–200 μL and 200–1000 μL. Each sample reached a 2 mL total volume in a sealed clear glass vial. Raman measurements were directly carried out through it. Judging from the material used and the experimental procedure, uncertainty on concentrations was found to reach 5% at worst.

Instrumentation

Raman spectra were recorded at stabilized room temperature (19 °C) with a Labram HR800 Raman spectrometer from Horiba Jobin-Yvon. The 691 nm wavelength of an Ondax laser diode was used. The laser beam was focused through a ×10 objective. Scattered radiation was collected at 180° relative to the excitation beam and detected with an Andor CCD cooled by the Peltier effect. A 300 lines mm^{-1} grating coupled to the spectrograph configuration allowed a spectral resolution of around 4 cm^{-1}. Spectral calibration was performed on a crystalline silicon sample using the known band at 520 cm^{-1}. Acquisition parameters were 5× 3 s from 200 cm^{-1} to 3400 cm^{-1} with 15 mW power for the sample.

Chemometrics

Band shifts appearing with time were corrected thanks to a homemade MatLab program. Indeed this could improve the ability prediction of chemometrics as shown by Witjes *et al.*[50] In addition to this, an algorithm was programmed in MatLab 7.0.1 to remove the Raman spectral background in a similar way for all of the spectra while keeping the analytical signal intact[51] (example in Fig. 1). This was possible by minimizing the following S function:

$$S = \sum_{(i)} \kappa_i (y_i - z_i)^2 + \lambda \sum_{(i)} (\Delta^2 z_i)^2 \quad (1)$$

with y the signal intensity for each i wavenumber, z the baseline, λ the smoothing parameter and p the asymmetric one as $\kappa_i = p$ if $y_i > z_i$ and $\kappa_i = 1 - p$ otherwise. The last term was defined as follows:

$$\Delta^2 z_i = (z_i - z_{i-1}) - (z_{i-1} - z_{i-2}) \quad (2)$$

The spectra were processed in two parts. Below 380 cm^{-1}, the two parameters needed for the calculations were $p = 10^{-1}$ and $\lambda = 10^2$. Above 380 cm^{-1}, $p = 10^{-4}$ and $\lambda = 10^5$. An example of this background treatment is shown in Fig. 1 applied on pure *meta*-xylene spectra. All of the presented following spectra have undergone the same background correction. Spectral identification and quantification were achieved using the SIMPLISMA algorithm[49] which was modified to automate data processing thanks to MatLab 7.0.1 again. As each different

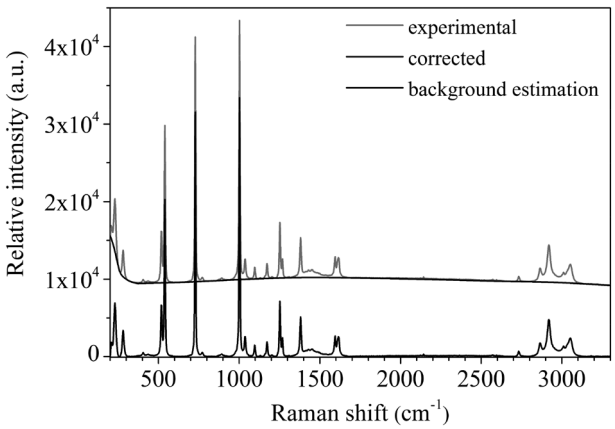

Fig. 1 Raman spectrum of experimental pure *meta*-xylene, calculated background and corresponding background-removed spectrum.

chemical could be distinguished from the other thanks to their principal Raman bands, the SIMPLISMA algorithm was able to extract the pure spectrum of each compound from a series of measured spectra whose signals were the result of the contributions from the different compounds. The general equation used by SIMPLISMA was the following:

$$D = CP + E \tag{3}$$

with D the experimental data matrix, C the contribution matrix, proportional to the concentration, P the pure variable matrix containing the pure spectra, and E the residual error matrix. The determination of pure variables was built on the following equation:

$$p_{i,k} = (w_{i,k}\sigma_i)/(\mu_i + \alpha) \tag{4}$$

with $p_{i,k}$ the purity value of the variable i from which the k^{th} pure variable is selected, μ_i and σ_i the mean and standard deviation of variable i. An offset α was added to give variables with a low mean value a lower purity value (noise range). The weight factor $w_{i,k}$ was a determinant-based function that corrected for previously chosen pure variables. First, the Q dispersion matrix was calculated from $D(\lambda)$ whose data were scaled by the length to give an equal contribution for each variable. So $D(\lambda)$ was given by:

$$d(\lambda)_{i,j} = d_{i,j}/(\mu_i{}^2 + (\sigma_i + \alpha)^2)^{1/2} \tag{5}$$

Then the dispersion matrix was:

$$Q = (1/n)D(\lambda)D(\lambda)^{\mathrm{T}} \tag{6}$$

with n the number of spectra. The determinants were finally calculated according to eqn (7):

$$w_{i,k} = \begin{vmatrix} Q_{i,i} & Q_{i,P_1} & \cdots & Q_{i,P_{k-1}} \\ Q_{P_1,i} & Q_{P_1,P_1} & \cdots & Q_{i,P_{k-1}} \\ \cdots & \cdots & \cdots & \cdots \\ Q_{P_{k-1},i} & \cdots & \cdots & Q_{P_{k-1},P_{k-1}} \end{vmatrix} \tag{7}$$

with P_1 the first pure variable. The index i was the variable for which the determinant was calculated. The index k indicated the index of the pure variable for which this determinant was calculated. After a successful data processing, when residual error Δ was minimized according to eqn (8), the relative contributions of the different species were given as well as their assigned pure spectra.

$$\Delta = \sqrt{\frac{\sum_{i=1}^{n_{\text{spec}}}\sum_{j=1}^{n_{\text{var}}}(d_{i,j} - d_{i,j}^{\text{calc}})^2}{\sum_{i=1}^{n_{\text{spec}}}\sum_{j=1}^{n_{\text{var}}} d_{i,j}{}^2}} \tag{8}$$

In eqn (8) above, $d_{i,j}$ was the i^{th} row and j^{th} column element of D; $d_{i,j}^{\text{calc}}$ was the i^{th} row and j^{th} column element of D calculated by the SIMPLISMA algorithm; n_{spec} was the number of mixture spectra and n_{var} was the number of recorded intensities. Next, each calculated pure spectrum had to be assigned to a single or a mixture of molecular species: such assignment

Table 1 Position of main Raman bands of BTEX in cm^{-1} (see ref. 35 for assignments)[a]

Benzene	Toluene	Ethylbenzene	*ortho*-Xylene	*meta*-Xylene	*para*-Xylene
	220 (m)		259 (m)	230 (s)–281 (m)	315 (m)
		490 (w)	508 (m)	519 (m)	461 (s)
610 (w)	524 (m)–624 (w)	624 (w)	585 (s)	540 (s)	647 (m)
	789 (s)	754 (sh)–772 (s)	737 (s)	726 (s)	
		968 (w)	988 (m)		813 (m)–831 (s)
994 (vs)	1006 (vs)	1006 (vs)		1003 (s)–1037 (w)	
1180 (w)	1033 (s)	1033 (s)–1067 (w)	1055 (s)	1097–1173 (w)	1185 (w)
	1212–1381 (m)	1205 (s)	1225 (s)	1253 (m)–1268 (w)	1207 (s)
			1387 (m)	1381 (m)	1381 (m)
1589–1609 (w)	1589–1607 (d)	1585 (sh)–1608 (m)	1584 (w)–1610 (m)	1594 (w)–1615 (w)	1620 (m)
	2869 (w)	2877 (w)	2860–2880 (w)	2865 (w)	2866 (w)
	2920 (w)	2904 (w)–2936 (m)	2920 (m)–2943 (sh)		2921 (m)
	2982 (w)	2966–2981 (w)	2979 (w)	2920 (m)	3015 (w)
3048 (sh)	3035 (sh)	3003–3037 (w)	3046 (m)	3010 (w)	3030 (w)
3063 (w)	3057 (m)	3055–3065 (m)	3080 (w)	3053 (w)	3055 (m)

[a] vs: very strong, s: strong, m: medium, w: weak, sh: shoulder.

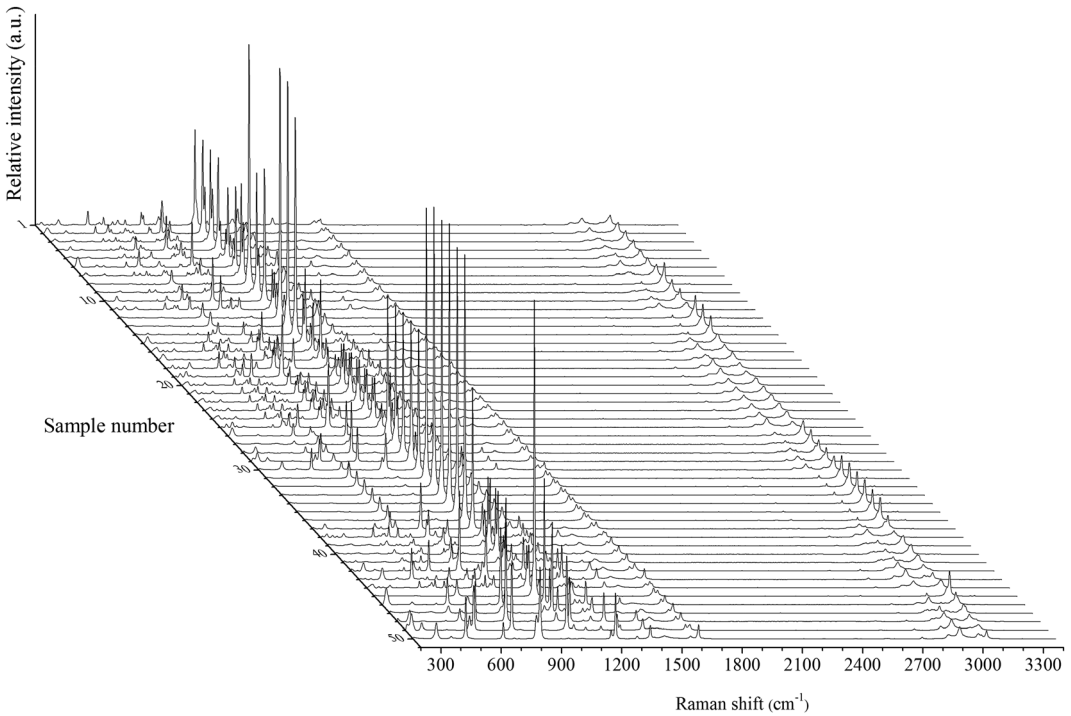

Fig. 2 Raman spectra of the different prepared samples: input data matrix for algorithm process.

was done using literature data or the Raman spectra measured on pure isolated analytes. Some supplementary programming was achieved to succeed in automatically identifying and quantifying the different known pollutants thanks to our own database while isolating the other molecules (for real cases).

Results and discussion

Spectra description

Herein different mixtures of the 6 exclusive BTEX compounds have mainly been carried out. Their Raman characteristic bands are listed in Table 1. The concentrations values, expressed in g L^{-1}, have been chosen to simulate the most unfavourable conditions and to test the limits of the chemometric process. In such a study, unfavourable conditions stand for a large gap of concentrations, multiple compounds with similar analytical responses, and one or several pollutants taking precedence over one or several remaining ones. The detailed description of the samples is given in Tables S-1 and S-2 of the ESI† while corresponding Raman spectra are shown in Fig. 2.

Advantages of SIMPLISMA method

From these spectra it can be noted that band covering is significant, so we can expect some difficulties in component discrimination. Moreover it is noteworthy that the whole spectra – from 200 to 3400 cm^{-1} – is used for this data processing

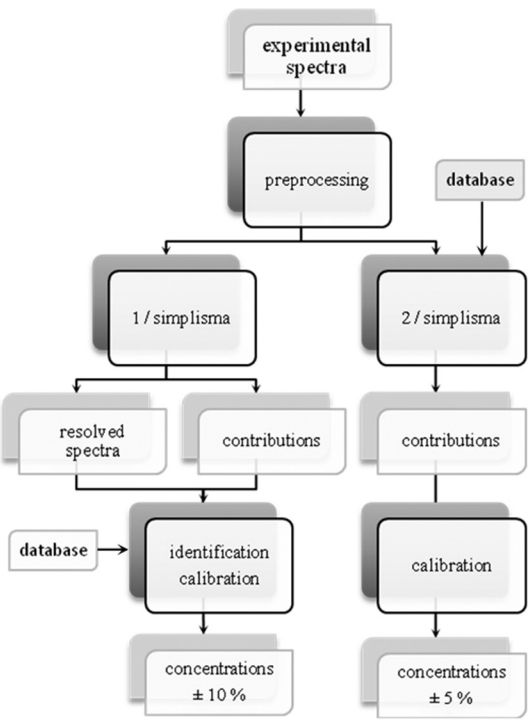

Chart 1 Data processing methodology and comparison between two ways: (1) the most upgradeable, (2) the most accurate.

whereas only some limited spectral parts are often used for other treatment.[30,31,48] As a consequence these methods are carried out in several steps while our algorithm enables the utilization of the whole information contained in spectra at once by the user.

Contrary to other methods, especially Multivariate Curve Resolution-Partial Least Square (MCR-PLS), Asymmetrical Least Square (ALS) or Classical Least Square (CLS), which are intensively used, the SIMPLISMA approach does not need an initial estimation of either component spectra or contribution profile. This is a huge advantage in sensor applications where the concentrations values are unknown and time- and space-dependent.

In addition to this, there is no need to build any set of calibrations, which is very time consuming and should be done for each matrix change. A simple database would be enough to enable the quantification. By definition, target pollutants are well-defined and well-known. The most dangerous among them for health and environment are even rightly indexed in law documents.[2–4]

Proceeding further, the spectral signature of one or several unexpected molecules could be separated from the known signals thanks to the versatility of the data treatment. With regard to the fifty or so samples, their Raman spectra (Fig. 2) have been input in our MatLab program described in Chart 1. Then two adjustable parameters must be specified, which are the number of components to be extracted and an offset value contributing to the reduction of the spectral noise in the computation. The following results have been obtained by setting the number of components to 6 and the offset value to 5% or

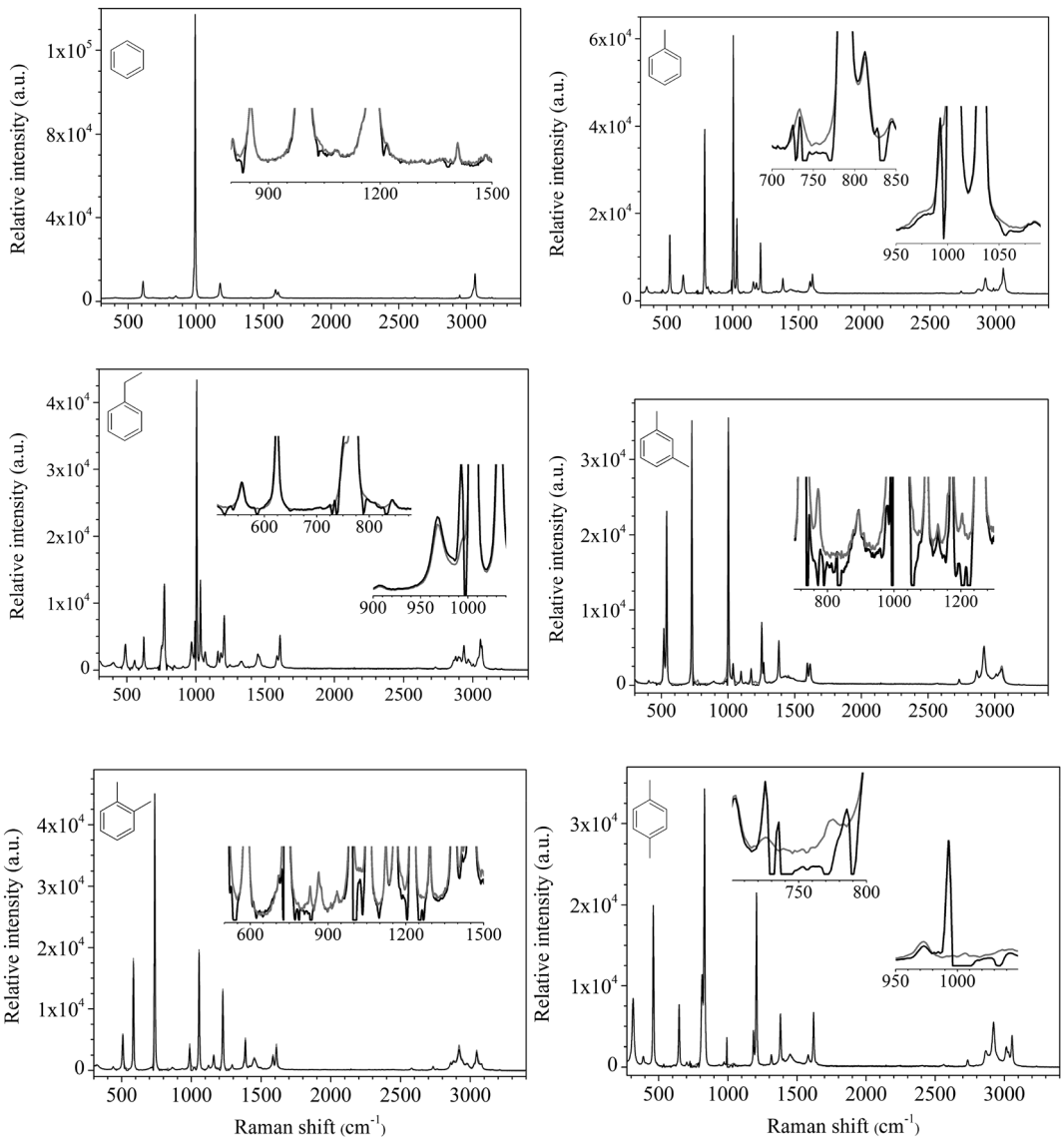

Fig. 3 Raman spectra of benzene, toluene, ethylbenzene, *meta*-xylene, *ortho*-xylene and *para*-xylene: comparison between pure experimental (grey) and resolved (black) spectra. Enlargements of interest are included into graphs.

less. Fig. 3 shows the 6 resolved spectra which match very well the 6 experimental spectra of each pure BTEX. Only enlargements can reveal the differences between the resolved and experimental BTEX spectra. The main mismatch comes from the 1000 cm^{-1} area where bands can be cut or added depending on each case. Thanks to their experimental pure spectra, we have implemented the identification and quantification of the pollutants in our algorithm. Even more, to improve result accuracy, we forced the algorithm to use experimental pure spectra instead of the resolved ones to split up the mixture spectral data (Chart 1, SIMPLISMA 2 way).

Comparison of the calculated and experimental spectra

In order to estimate the agreement of the calculations with the expected quantities, we have plotted the computed concentrations *versus* the actual ones (Fig. 4). As highlighted by these plots, the values fit well and even better than ref. 31. One more fact to underline is the variation in accuracy which seems to be dependent on the spectral characteristics of each BTEX. Sample preparation uncertainty was calculated by adding those given by the providers of the equipment used and reached 5%. Spectral uncertainty was determined by using the standard deviation σ of the peak maximum from each spectrum measured 10 times on the same sample. Five random samples were used to reach an uncertainty of 15% thanks to the formula $100(3\sigma/\max(\text{peak}))$.

From all the results (see also ESI Tables S-1 and S-2 and Fig. S-2†) and taking into consideration the previous uncertainties, data processing error is estimated to reach 5% (according to relative deviations) when the Raman signal of a component contributes more than 10% of the total signal. Below this value, uncertainty can reach up to 10% and when

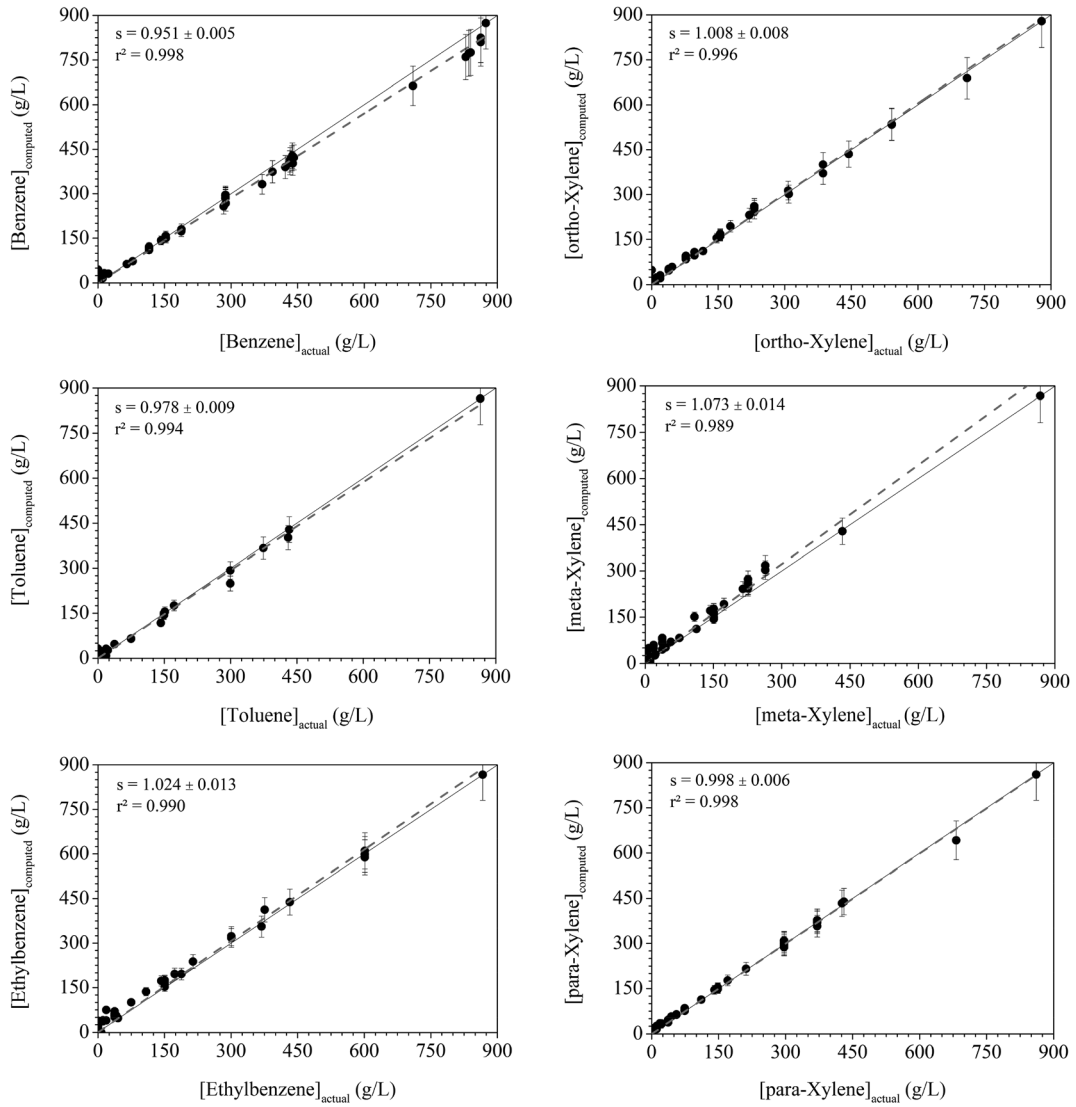

Fig. 4 Plots of computed *vs.* actual concentrations of BTEX compounds in different mixtures and linear fitting (grey dash) with the slope s and the correlation coefficient r^2.

the signal contribution of one species is less than 2%, error is out of tolerance. This can be realized thanks to Fig. 4 where computed *versus* actual concentrations of BTEX have been plotted. A perfect matching should result in a linear trend with a slope of 1 and an intercept of 0. This can be compared to the linear fit included in the Fig. 4 – with intercepts fixed at 0. Inaccuracy is mainly caused by spectral covering. Indeed from Table 1 and Fig. 3 we can note many common bands between BTEX spectra, particularly around 1000 cm^{-1}. Now each BTEX compound exhibits a Raman signal in this spectral area, except for *para*-xylene whose concentration is consequently the most accurately determined as shown in Fig. 4. In the same way, *ortho*-xylene exhibits a very low signal in this area, so a very good computation is carried out. Logically, benzene with its only intense characteristic band at 994 cm^{-1} is determined with the worst accuracy, being consistently underestimated. In continuation, the higher dispersion of values below 100 g L^{-1} tends to raise another source of inaccuracy. Indeed big proportion gaps between the components cause determination gaps between the lowest computed and actual values.

Data processing adaptability

An 'unknown' pollutant was then added in order to test the data processing adaptability. The program was run incrementing the component number and succeeded in identifying and quantifying the known BTEX as previously.

The remaining unknown signal has been isolated in one more resolved spectrum and the corresponding contribution. This enables a qualitative estimation of its proportion in the samples. To proceed further, we have to assign the resolved spectrum to a known molecule. Here we can continue by noting that the characteristic computed bands match the chloroform ones (Fig. 5). Again the presence of a parasite residual signal around 1000 cm^{-1} in the resolved spectrum can be noticed. Including the chloroform pure spectrum in our program database allows us to quantify $CHCl_3$. Actually we have introduced chloroform in two samples among BTEX, 60 and 393 g L^{-1} (see ESI Table S-2†). Computed values have been found to be 66 and 406 g L^{-1}, which are very close to the expected amounts. These results show that the processing method is upgradeable.

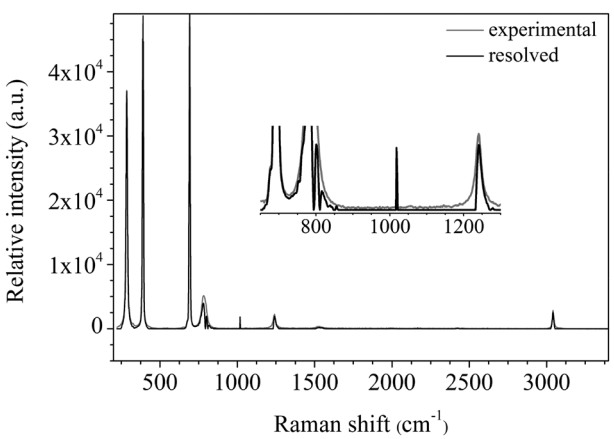

Fig. 5 Comparison between experimental (gray) and resolved (black) Raman spectra of chloroform. Enlargement of interest is included into graph.

Conclusions

The amounts of each BTEX species can be predicted in a wide concentration range by processing Raman data thanks to the SIMPLISMA algorithm model. With the integration of a database better accuracy is obtained (5%), above all regarding the lower concentration values. This method is efficient even in the case of big gaps such as 1‰ between the minimum and maximum analyte concentration. However in that situation accuracy becomes lower. The presence of an 'unknown' compound different from BTEX in its structure as well as its chemical nature was simulated by adding chloroform in mixtures. Its spectral fingerprint was successfully extracted. Then it was embedded in the database to succeed in determining its amount. Thus this is a fast, upgradeable data processing method with good accuracy suitable for sensor applications.

Conflict of interest

The authors declare no competing financial interest.

Acknowledgements

This project was financed by ANR, the French Research Agency, thanks to the ECOTECH 2011 program, through the ANR-11-ECOT-010-REMANTAS project.

Notes and references

1 S. J. Lawrence, in *Description, properties, and degradation of selected organic volatile compounds detected in ground water – A review of selected literature*, U. S. Geological Survey, 2006, http://pubs.usgs.gov/ofr/2006/1338.
2 US Environmental Protection Agency, *Federal Register*, 1984, Method 624, 141.
3 Directive 2000/60/EC of the European Parliament and of the Council of 23 October 2000, Official Journal of the European Communications, 327, 22 December 2002.
4 World Health Organization, *'Guidelines for Drinking Water Quality'*, 3rd edn, Geneva, 2008.
5 A. Picot and F. Montandon, in *'Ecotoxicochimie appliquée aux hydrocarbures'*, Tec & Doc Lavoisier, 2013, pp. 291–342.
6 D. E. C. Mazzeo, S. T. Matsumoto, C. E. Levy, D. de Franceschi de Angelis and M. A. Marin-Morales, *Chemosphere*, 2013, **90**, 1030–1036.
7 L. Arthur, L. M. Killam, S. Motlagh, M. Lim, D. W. Potter and J. Pawliszyn, *Environ. Sci. Technol.*, 1992, **26**, 979–983.

8 A. Serrano and M. Gallego, *J. Chromatogr., A*, 2004, **1045**, 181–188.
9 D. Sciarrone, P. Quinto Tranchida, C. Ragonese, L. Schipilliti and L. Mondello, *J. Sep. Sci.*, 2010, **33**, 594–599.
10 S. M. Pyle and M. G. Donald, *Talanta*, 1994, **41**, 1845–1852.
11 R. Kubinec, J. Adamuščin, H. Jurdáková, M. Foltin, I. Ostrovský, A. Kraus and L. Soják, *J. Chromatogr., A*, 2005, **1084**, 90–94.
12 A. Neves Fernandes, C. Duarte Gouveia, M. Tadeu Grassi, J. da Silva Crespo and M. Giovanela, *Bull. Environ. Contam. Toxicol.*, 2014, **92**, 455–459.
13 S. Lacorte, L. Olivella, M. Rosell, M. Figueras, A. Ginebreda and D. Barceló, *Chromatographia*, 2002, **56**, 739.
14 J. C. Flórez Menéndez, M. L. Fernández Sánchez, J. E. Sánchez Uría, E. F. Martínez and A. Sanz-Medel, *Anal. Chim. Acta*, 2000, **415**, 9.
15 Z. Wang, K. Li, M. Fingas, L. Sigouin and L. Ménard, *J. Chromatogr., A*, 2002, **971**, 173–184.
16 A. Alonso, M. A. Fernández-Torroba, M. T. Tena and B. Pons, *Chromatographia*, 2003, **57**, 369.
17 M. Farajzadeh and A. Mardani, *Anal. Sci.*, 2001, **17**, 1059–1062.
18 A. Esteve-Turillas, S. Armanta, S. Garrigues, A. Pastor and M. de la Guardia, *Anal. Chim. Acta*, 2007, **587**, 89–96.
19 Y. Alsalka, F. Karabet and S. Hashem, *Anal. Methods*, 2010, **2**, 1026–1035.
20 G. Y. A. Tan, C. L. Chen, L. Zhao, Y. Mo, V. W. C. Chang and J. Y. Wang, *Anal. Methods*, 2012, **4**, 3545–3550.
21 B. L. Wittkamp and D. C. Tilotta, *Anal. Chem.*, 1995, **67**, 600–605.
22 K. J. Ewing, G. Nau, T. Bilodeau, D. M. Dagenais, F. Buchholtz and I. D. Aggarwal, *Anal. Chim. Acta*, 1997, **340**, 227–232.
23 W. A. Chudyk, M. M. Carrabba and J. E. Kenny, *Anal. Chem.*, 1985, **57**, 1237–1242.
24 M. Karlowatz, M. Kraft and B. Mizaikoff, *Anal. Chem.*, 2004, **76**, 2643–2648.
25 B. Pejcic, L. Boyd, M. Myers, A. Ross, Y. Raichlin, A. Katzir, R. Lu and B. Mizaikoff, *Org. Geochem.*, 2013, **55**, 63–71.
26 J. A. Sorensen and L. C. Thompson, *Anal. Chem.*, 1985, **57**, 1087–1091.
27 T. Jawhari, P. J. Hendra, H. A. Willis and M. Judkins, *Spectrochim. Acta, Part A*, 1990, **46**, 161–170.
28 S. A. Asher, *Anal. Chem.*, 1993, **65**, 201–210.
29 Q. Ye, Q. Xu, Y. Yu, R. Qu and Z. Fang, *Opt. Commun.*, 2009, **282**, 3785–3788.
30 A. O'Grady, A. C. Dennis, D. Denvir, J. J. McGarvey and S. E. J. Bell, *Anal. Chem.*, 2001, **73**, 2058–2065.
31 J. B. Cooper, K. L. Wise, W. T. Welch, M. B. Sumner, B. K. Wilt and R. R. Bledsoe, *Appl. Spectrosc.*, 1997, **51**, 1613–1620.
32 C. M. Stellman, K. J. Ewing, F. Buchholtz and I. D. Aggarwal, *Sens. Actuators, B*, 1998, **53**, 173–178.
33 H. Parastar, M. Jalali-Heravi and R. Tauler, *Trends Anal. Chem.*, 2012, **31**, 134–143.
34 J. H. Giles, D. A. Gilmore and M. B. Denton, *J. Raman Spectrosc.*, 1999, **30**, 767–771.
35 S. K. Sharma, A. K. Misra and B. Sharma, *Spectrochim. Acta, Part A*, 2005, **61**, 2404–2412.
36 K. Carron, L. Peltersen and M. Lewis, *Environ. Sci. Technol.*, 1992, **26**, 1950–1954.
37 J. S. Cooper, M. Myers, E. Chow, L. J. Hubble, J. M. Cairney, B. Pejcic, K.-H. Müller, L. Wieczorek and B. Raguse, *J. Nanopart. Res.*, 2014, **16**, 2173–2186.
38 O. Péron, E. Rinnert, M. Lehaitre, P. Crassous and C. Compère, *Talanta*, 2009, **79**, 199–204.
39 O. Péron, E. Rinnert, T. Toury, M. Lamy de la Chapelle and C. Compère, *Analyst*, 2011, **136**, 1018–1022.
40 J. Pfannkuche, L. Lubecki, H. Schmidt, G. Kowalewska and H.-D. Kronfeldt, *Mar. Pollut. Bull.*, 2012, **64**, 614–626.
41 X. Shi, Y.-H. Kwon, J. Ma, R. Zheng, C. Wang and H.-D. Kronfeldt, *J. Raman Spectrosc.*, 2013, **44**, 41–46.
42 J. B. Cooper, *Chemom. Intell. Lab. Syst.*, 1999, **56**, 231–247.
43 L. Mutihac and R. Mutihac, *Anal. Chim. Acta*, 2008, **612**, 1–18.
44 C. Ruckebusch and L. Blanchet, *Anal. Chim. Acta*, 2013, **765**, 28–36.
45 B. Pejcic, M. Myers and A. Ross, *Sensors*, 2009, **9**, 6232–6253.
46 P. E. Flecher, J. B. Cooper, T. M. Vess and W. T. Welch, *Spectrochim. Acta, Part A*, 1996, **52**, 1235–1244.
47 Y. B. Monakhova, S. A. Astakhov, A. Kraskov and S. P. Mushtakova, *Chemom. Intell. Lab. Syst.*, 2010, **103**, 108–115.
48 X. Zhang, X. Qi, M. Zou and J. Wu, *J. Raman Spectrosc.*, 2012, **43**, 1487–1491.
49 W. Windig, *Chemom. Intell. Lab. Syst.*, 1997, **36**, 3–16.
50 H. Witjes, M. van den Brink, W. J. Melssen and L. M. C. Buydens, *Chemom. Intell. Lab. Syst.*, 2000, **52**, 105–116.
51 P. H. C. Eilers, *Anal. Chem.*, 2003, **75**, 3631–3636.
52 R. Fischer, K. M. Hanson, V. Dose and W. von der Linden, *Phys. Rev. E*, 2000, **61**, 1152–1160.
53 S. G. Razul, W. J. Fitzgerald and C. Andrieu, *Nucl. Instrum. Methods Phys. Res., Sect. A*, 2003, **497**, 492–510.
54 V. Mazet, C. Carteret, D. Brie, J. Idier and B. Humbert, *Chemom. Intell. Lab. Syst.*, 2005, **76**, 121–133.
55 N. N. Brandt, O. O. Brovko, A. Y. Chikishev and O. D. Paraschuk, *Appl. Spectrosc.*, 2006, **60**, 288–293.
56 Z.-M. Zhang, S. Chen, Y.-Z. Liang, Z.-X. Liu, Q.-M. Zhang, L.-X. Ding and F. Ye, *J. Raman Spectrosc.*, 2009, **41**, 659–669.
57 A. E. Kandjani, M. J. Griffin, R. Ramanathan, S. J. Ippolito, S. K. Bhargava, V. Bansal and H. Zhou, *J. Raman Spectrosc.*, 2013, **44**, 608–621.
58 X. Liu, Z. Zhang, Y. Liang, P. F. M. Sousa, Y. Yun and L. Yu, *Chemom. Intell. Lab. Syst.*, 2014, **139**, 97–108.